Mathematics and Mechanics of Solids OnlineFirst, published on September 17, 2008 as doi:10.1177/1081286508092010

Spontaneous Cavitation in Growing Elastic Membranes

JOSEPH MCMAHON
Program in Applied Mathematics, University of Arizona, AZ 85721, USA

ALAIN GORIELY
MICHAEL TABOR
Program in Applied Mathematics and Department of Mathematics, University of Arizona, AZ 85721, USA

(Received 20 March 2008; accepted 25 March 2008)

Abstract: One of the possible effects of volumetric growth in elastic materials is the creation of residual stresses. These stresses are known to change many of the classical properties of the material and have been studied extensively in the context of volumetric growth in biomechanics. Here we consider the problem of elastic cavitation in a growing compressible elastic membrane. Growth is taken to be homogeneous but anisotropic, and the membrane is assumed to remain axisymmetric during growth and deformation. We prove that neo-Hookean membranes cannot cavitate, but for Varga elastic materials we find conditions under which the material exhibits spontaneous cavitation in the absence of external loads, in marked distinction from the cavitation problem without growth.

Key Words: elasticity, growth, cavitation

1. INTRODUCTION

When an elastic body swells or grows, different volume elements may be subject to deformations that differ in such a way that the integrity of the body may be compromised and, as a result, stresses develop to prevent the non-physical overlapping of material elements. These so-called *residual stresses* [1], found in most soft biological structures, are known to change the material properties and behaviors under loads. For instance, residual stresses regulate transmural stress gradients in arteries [2, 3], and they can spontaneously destabilize growing or shrinking spherical shells [4, 5]. Here we consider, in the context of elastic membranes, the possible rôle of growth in triggering cavity formation.

Elastic cavitation is the mechanism by which an empty cavity forms inside an elastic solid under tension. Pioneering experimental and theoretical work on this topic is due to Gent and Lindley, who studied rupture in rubber cylinders [6]. In a seminal paper, Ball [7] put the subject on a solid mathematical foundation in the context of finite hyperelasticity. In particular, he transformed the analysis into a bifurcation problem by showing that a neo-Hookean sphere under hydrostatic load supports both trivial (with no inner cavity) and

Mathematics and Mechanics of Solids **00:** 000–000, 2008 DOI: 10.1177/1081286508092010

Los Angeles, London, New Delhi and Singapore

cavitated solutions for a load exceeding $5E/6$ (where E is Young's modulus of infinitesimal deformations). Following Ball's work, cavitation bifurcations and solutions have been studied for a variety of specific strain energy densities, geometries, loads, and constraints [8–15], and further experimental and numerical works have validated the theoretical approaches of some of these theories [16–18]. However, the role of elastic cavitation as a mechanism for fracture initiation remains a controversial topic.

Elastic cavitation has also been studied for membranes. Interestingly, depending on the modeling assumptions on the membrane, cavitation may not be possible [19]. More precisely, in a model of a Varga elastic membrane where thickness is negligible compared to the smallest curvature of the "middle surface" of the membrane, no cavitated solution exists [20]. However, if the membrane is considered to be a true two-dimensional object (i.e of zero thickness), cavitation is possible [21, 22]. It is now particularly interesting to study the case of a membrane subject to growth and see if it allows for the existence of cavitated solutions—a drastic change of basic material behavior.

To include growth into the theory of elasticity, we follow the prescription of Rodriguez et al. [23] for volumetric growth and assume that the geometric deformation tensor can be decomposed into the product of an elastic deformation tensor and a growth tensor. The local expansion or contraction of volume due to the addition or loss of mass is expressed by the growth tensor, and the elastic deformation tensor describes the mechanical response of the material to maintain material compatibility and integrity. When this decomposition is adopted in finite hyperelasticity, the stresses depend on the elastic deformation alone. This theory of growth has been applied to many different systems in biology [24–33] and has been further developed theoretically by a number of authors [34–37].

The paper is organized as follows. In Section 2, we describe the kinematics of growth and how to adapt the theory of axisymmetric elastic membranes to include growth. In Section 3, we prove that neo-Hookean compressible axisymmetric membranes cannot cavitate for anisotropic and homogeneous growth. In Section 4, we study growing Varga membranes and restrict our attention to a particular class of compressible materials for which we find conditions for the existence of cavitated solutions. These solutions are then computed explicitly by numerical integration.

2. ELASTICITY WITH GROWTH

2.1. Kinematics of Growth

The deformation of a material body is given by $\mathbf{x} = \boldsymbol{\chi}(\mathbf{X})$, where $\mathbf{X}$ and $\mathbf{x}$ describe the material coordinates of a point in the reference configuration and in the current configuration, respectively. Then $\mathbf{F} = \partial\mathbf{x}/\partial\mathbf{X}$ is the *geometric* deformation gradient. Following [23], we incorporate growth into elasticity via the multiplicative decomposition of the deformation gradient. The deformation gradient $\mathbf{F}$ is assumed to be equal to the product $\mathbf{A} \cdot \mathbf{G}$, where $\mathbf{G}$ is the *growth tensor* (field) describing locally the change in configuration due to non-elastic volumetric growth, and $\mathbf{A}$ is a tensor (field) that describes the local elastic deformation that arises in response to growth and applied forces.

While the product $\mathbf{F} = \mathbf{A} \cdot \mathbf{G}$ is a true deformation gradient, if either $\mathbf{A}$ or $\mathbf{G}$ is not a true deformation gradient, then the other is also not a deformation gradient. In this case, $\mathbf{G}$ and $\mathbf{A}$ have the following physical interpretations:

- $\mathbf{G}$ describes how growth would deform a small amount of matter if it were not confined or otherwise influenced by the presence of neighboring matter.
- $\mathbf{A}$ describes a "grown" neighborhood's subsequent elastic deformation to accommodate the presence of neighboring matter and the influence of applied forces.

2.2. *Hyperelasticity*

If the material is hyperelastic, then the strain energy density depends only on $\mathbf{A}$, the elastic component of the deformation gradient. In a membrane theory, we consider a thin sheet of elastic material whose "middle surface" has negligible curvature and whose mechanical properties are uniform through the (small) thickness of the sheet. Therefore, it is reasonable to introduce thickness-averaged quantities (denoted by overbars). For instance, we denote by $\overline{W} = \overline{W}(\mathbf{A})$ the elastic strain energy per unit volume. The (thickness-averaged) nominal stress tensor is then

$$\overline{\mathbf{S}} = (\det \mathbf{G}) \, \frac{\partial}{\partial \mathbf{F}} \overline{W}(\mathbf{A}) = (\det \mathbf{G}) \, \mathbf{G}^{-1} \cdot \overline{W}_{\mathbf{A}}, \tag{2.1}$$

and the Cauchy stress tensor is

$$\begin{aligned} \overline{\boldsymbol{\sigma}} &= (\det \mathbf{F})^{-1} \, \mathbf{F} \cdot \overline{\mathbf{S}} \\ &= (\det \mathbf{A})^{-1} \, (\det \mathbf{G})^{-1} \, (\det \mathbf{G}) \, \mathbf{A} \cdot \mathbf{G} \cdot \mathbf{G}^{-1} \cdot \overline{W}_{\mathbf{A}} \\ &= (\det \mathbf{A})^{-1} \, \mathbf{A} \cdot \overline{W}_{\mathbf{A}}. \end{aligned} \tag{2.2}$$

2.3. *An Axisymmetric Membrane Model*

Using thickness-averaged quantities and assuming axial symmetry, we adopt Haughton and Ogden's model [19, 38] for an axisymmetric membrane. In this case the three principal stretches are

$$\lambda_1 = \frac{\mathrm{d}r}{\mathrm{d}R}, \quad \lambda_2 = \frac{r}{R}, \quad \lambda_3 = \frac{h}{H}, \tag{2.3}$$

where $R, \ H$ are the radius and thickness at a point on the membrane in the reference configuration, and $r, \ h$ are the corresponding radius and thickness in the current configuration. Cauchy's equation for the stress tensor reduces to a single equation

$$\frac{1}{h} \frac{\mathrm{d}}{\mathrm{d}r} \left(h \overline{\sigma}_{11} \right) + \frac{\overline{\sigma}_{11} - \overline{\sigma}_{22}}{r} = 0, \tag{2.4}$$

together with the "plane stress" condition:

$$\overline{\sigma}_{33} = 0. \tag{2.5}$$

Here, $\overline{\sigma}_{11}$ is the radial Cauchy stress, $\overline{\sigma}_{22}$ is the azimuthal Cauchy stress, and $\overline{\sigma}_{33}$ is the Cauchy stress normal to the middle surface of the sheet. These stresses are derived from a thickness-averaged strain energy density $\overline{W}$ via Equation (2.2).

If we assume constant thickness H of the reference configuration, then Equation (2.4) simplifies to

$$\frac{1}{\lambda_3}\frac{\mathrm{d}}{\mathrm{d}r}(\lambda_3\overline{\sigma}_{11}) + \frac{\overline{\sigma}_{11} - \overline{\sigma}_{22}}{r} = 0. \tag{2.6}$$

Since this model assumes minimal curvature of the membrane's middle surface, $r = r(R)$ is a monotonically increasing function. Thus Equation (2.6) can be re-written as

$$\frac{1}{\lambda_3}\left(\frac{\mathrm{d}r}{\mathrm{d}R}\right)^{-1}\frac{\mathrm{d}}{\mathrm{d}R}(\lambda_3\overline{\sigma}_{11}) + \frac{\overline{\sigma}_{11} - \overline{\sigma}_{22}}{r} = 0, \tag{2.7}$$

or

$$\frac{1}{\lambda_3\lambda_1}\frac{\mathrm{d}}{\mathrm{d}R}(\lambda_3\overline{\sigma}_{11}) + \frac{\overline{\sigma}_{11} - \overline{\sigma}_{22}}{r} = 0, \tag{2.8}$$

where all quantities are now considered to be functions of R.

2.4. Growth in Elastic Membranes

Here we consider a simple case of growth that is homogeneous and anisotropic in the plane of the middle surface, with no growth perpendicular to that surface. The principal stretches of the deformation gradient are then

$$\gamma_1\lambda_1 = \frac{\mathrm{d}r}{\mathrm{d}R}, \quad \gamma_2\lambda_2 = \frac{r}{R}, \quad \lambda_3 = \frac{h}{H}, \tag{2.9}$$

where γ_1 and γ_2 are constant growth parameters. We assume constant thickness of the reference configuration, so H is also constant. Since $\mathrm{d}r/\mathrm{d}R$ has a different form when growth is included, Equation (2.8) is changed to

$$\frac{1}{\lambda_3\gamma_1\lambda_1}\frac{\mathrm{d}}{\mathrm{d}R}(\lambda_3\overline{\sigma}_{11}) + \frac{\overline{\sigma}_{11} - \overline{\sigma}_{22}}{r} = 0, \tag{2.10}$$

where λ_1 has been replaced by $\gamma_1\lambda_1$. The first two nonzero components of the Cauchy stress have the forms

$$\overline{\sigma}_{11} = \frac{1}{\lambda_2\lambda_3}\frac{\partial\overline{W}}{\partial\lambda_1} \quad \text{and} \quad \overline{\sigma}_{22} = \frac{1}{\lambda_1\lambda_3}\frac{\partial\overline{W}}{\partial\lambda_2}, \tag{2.11}$$

while the plane stress condition ($\overline{\sigma}_{33} = 0$) is

$$\frac{1}{\lambda_1 \lambda_2} \frac{\partial \overline{W}}{\partial \lambda_3} = 0. \tag{2.12}$$

2.5. *Growth-Induced Cavitation*

We consider the possibility of spontaneous *growth-induced* cavitation. That is, we prescribe growth parameters and *zero* applied loads and then seek an axisymmetric deformed configuration such that $r(0) > 0$. Since the total radial traction at the cavity's surface is $2\pi r h \overline{\sigma}_{11}|_{R=0} = 2\pi r \lambda_3 H \overline{\sigma}_{11}|_{R=0}$ and since $r(0) > 0$, we impose the restriction

$$\lambda_3 \overline{\sigma}_{11}|_{R=0} = 0, \tag{2.13}$$

with the same boundary condition at $R = R_{\max}$. In the following sections we consider two types of elastic strain energy densities.

3. ABSENCE OF CAVITATION IN NEO-HOOKEAN MATERIAL

The compressible neo-Hookean strain energy density has the form

$$\overline{W}(\lambda_1, \lambda_2, \lambda_3) = \mu \left(\frac{1}{2} \left(\lambda_1^2 + \lambda_2^2 + \lambda_3^2 \right) - g(J) \right), \tag{3.1}$$

where μ is constant and $J = \det \mathbf{A} = \lambda_1 \lambda_2 \lambda_3$. From Equation (2.11), the pertinent components of the Cauchy stress are

$$\overline{\sigma}_{11} = \frac{\mu}{\lambda_2 \lambda_3} \left(\lambda_1 - \lambda_2 \lambda_3 g'(J) \right), \quad \overline{\sigma}_{22} = \frac{\mu}{\lambda_1 \lambda_3} \left(\lambda_2 - \lambda_1 \lambda_3 g'(J) \right), \tag{3.2}$$

and the plane stress condition, Equation (2.12), requires

$$\lambda_3^2 = J g'(J). \tag{3.3}$$

The equilibrium equation takes the form

$$\frac{1}{\lambda_3 \gamma_1 \lambda_1} \frac{\mathrm{d}}{\mathrm{d}R} \left(\lambda_3 \overline{\sigma}_{11} \right) + \frac{\mu}{r} \left(\frac{\lambda_1}{\lambda_2 \lambda_3} - \frac{\lambda_2}{\lambda_1 \lambda_3} \right) = 0, \tag{3.4}$$

so that

$$\frac{\mathrm{d}}{\mathrm{d}R} \left(\lambda_3 \overline{\sigma}_{11} \right) = \frac{\mu \gamma_1}{r} \left(\lambda_2 - \frac{\lambda_1^2}{\lambda_2} \right). \tag{3.5}$$

We consider two types of behavior as $R \to 0$: $\lambda_2 \gg \lambda_1$ and otherwise. The latter condition will be denoted $\lambda_1 \stackrel{\gg}{\sim} \lambda_2$, which indicates that, asymptotically, λ_1 grows at a rate greater than or equivalent to the rate of growth of λ_2.

3.1. $\boldsymbol{\lambda_2 \gg \lambda_1}$

We assume $\lambda_1 = \varepsilon \lambda_2$, where ε is continuous and $\varepsilon(R) \to 0$ as $R \to 0$. The equilibrium equation, Equation (3.5), can be re-written as

$$\begin{aligned}\frac{\mathrm{d}}{\mathrm{d}R}\left(\lambda_3 \overline{\sigma}_{11}\right) &= \frac{\mu \gamma_1}{r} \lambda_2 \left(1 - \varepsilon^2\right) \\ &= \frac{\mu \gamma_1}{r} \frac{r}{\gamma_2 R} \left(1 - \varepsilon^2\right) \\ &= \frac{\mu \gamma_1}{\gamma_2} \left(1 - \varepsilon^2\right) R^{-1}. \end{aligned} \tag{3.6}$$

Given $\delta \in (0, 1)$, for small-enough $R > 0$,

$$\frac{\mathrm{d}}{\mathrm{d}R}\left(\lambda_3 \overline{\sigma}_{11}\right) > \frac{\mu \gamma_1}{\gamma_2} \left(1 - \delta^2\right) R^{-1}, \tag{3.7}$$

so that for sufficiently small $R_2 > R_1 > 0$,

$$\lambda_3 \overline{\sigma}_{11}|_{R=R_2} - \lambda_3 \overline{\sigma}_{11}|_{R=R_1} > \frac{\mu \gamma_1}{\gamma_2} \left(1 - \delta^2\right) \ln \left(\frac{R_2}{R_1}\right). \tag{3.8}$$

If we fix R_2 and let $R_1 \to 0$, we see that the total force on the surface at $r(R_1)$ diverges. In this case a cavity cannot be sustained, even with (finite) nonzero radial traction at the inner radius.

3.2. $\boldsymbol{\lambda_1 \stackrel{\gg}{\sim} \lambda_2}$

In this case we let $\lambda_2 = \varepsilon \lambda_1$, where ε is continuous and

$$\lim_{R \to 0} \varepsilon(R) = \begin{cases} 0 & \text{if} \quad \lambda_1 \gg \lambda_2, \\ c > 0 & \text{if} \quad \lambda_1 \text{ and } \lambda_2 \text{ are on the same scale.} \end{cases}$$

The definitions in Equation (2.9) and the relation $\varepsilon \lambda_1 = \lambda_2$ imply

$$\frac{\varepsilon}{\gamma_1} \frac{\mathrm{d}r}{\mathrm{d}R} = \frac{r}{\gamma_2 R}, \tag{3.9}$$

so that, given any $\delta > 0$, for sufficiently small $R_2 > R_1 > 0$,

$$\int_{R_1}^{R_2} \frac{\mathrm{d}r}{r} = \frac{\gamma_1}{\gamma_2} \int_{R_1}^{R_2} \frac{\mathrm{d}R}{\varepsilon(R)R} > \frac{\gamma_1}{\gamma_2} \int_{R_1}^{R_2} \frac{\mathrm{d}R}{(c+\delta)R}. \tag{3.10}$$

Here $c = 0$ if $\lambda_1 \gg \lambda_2$. Integration yields

$$\ln\left(\frac{r(R_2)}{r(R_1)}\right) > \frac{\gamma_1}{\gamma_2(c+\delta)} \ln\left(\frac{R_2}{R_1}\right), \quad \text{or} \quad R_1^{\gamma_1/\gamma_2(c+\delta)} r(R_2) > R_2^{\gamma_1/\gamma_2(c+\delta)} r(R_1). \tag{3.11}$$

If we fix R_2 and let $R_1 \to 0$, we see that $r(R_1) \to 0$. Cavitation is precluded in this scenario, as well.

4. VARGA MATERIAL

In [11] Haughton proved that elastic materials with the Varga strain energy density (without volumetric growth) do not have cavitated configurations without radial traction at the cavity's surface. Here we show that for certain cases of anisotropic but homogeneous growth a particular class of Varga strain energy densities does permit cavitation in the absence of loading. The compressible Varga strain energy density has the form

$$\overline{W}(\lambda_1, \lambda_2, \lambda_3) = \mu\left(\lambda_1 + \lambda_2 + \lambda_3 - g(J)\right), \tag{4.1}$$

where μ is constant and $J = \lambda_1\lambda_2\lambda_3$. The Cauchy stresses are

$$\overline{\sigma}_{11} = \mu\left(\frac{1}{\lambda_2\lambda_3} - g'(J)\right) \quad \text{and} \quad \overline{\sigma}_{22} = \mu\left(\frac{1}{\lambda_1\lambda_3} - g'(J)\right), \tag{4.2}$$

and the plane-stress condition implies

$$\frac{1}{\lambda_1\lambda_2} = g'(J), \quad \text{or} \quad \lambda_3 = Jg'(J). \tag{4.3}$$

We impose three restrictions on the function g found in the strain energy density. First, since there should be no elastic energy in the absence of elastic deformation, we require $\overline{W}(1, 1, 1) = 0$, which implies $g(1) = 3$. Second, there should be no stress in the elastically unstrained state, so each partial derivative of $\overline{W}$ must be zero-valued when $\lambda_1 = \lambda_2 = \lambda_3 = 1$; this implies $g'(1) = 1$. Finally, the requirement of a positive bulk modulus in the unstrained state implies (see [39])

$$\frac{\lambda}{3}\frac{\mathrm{d}}{\mathrm{d}\lambda}\overline{\sigma}_{ii}(\lambda, \lambda, \lambda)\bigg|_{\lambda=1} > 0. \tag{4.4}$$

For the compressible Varga material, we have

$$-\frac{\mu}{3}\left(3g''(1)+2\right) > 0 = -\frac{\mu}{3}\left(2g''(1)+3\right) > 0. \tag{4.5}$$

and hence we require that $g''(1) < -2/3$.

4.1. An Equivalent ODE System

The equation of equilibrium and the plane stress condition can be converted into a pair of ordinary differential equations with independent variable R and dependent variables r and J (see the Appendix for the derivation).

$$\frac{\mathrm{d}J}{\mathrm{d}R} = \frac{\gamma_2 - \gamma_1}{rg'(J)\left(g'(J)+2Jg''(J)\right)} \tag{4.6}$$

$$\frac{\mathrm{d}r}{\mathrm{d}R} = \frac{\gamma_1\gamma_2 R}{rg'(J)} \tag{4.7}$$

where primes denotes differentiation with respect to function argument and where no argument is given prime refers to differentiation with respect to R. In light of these equations, we impose more restrictions on g. We want both J' and r' to remain finite within the material, so we require $g'(J)$ and $g'(J)+2Jg''(J)$ to remain nonzero. As such, both of these expressions have fixed sign within the material. Recall that $g'(1) = 1$ and $g''(1) < -2/3$; based on this, we assume that $g'(J)$ is positive for $J > 0$ and $g'(J)+2Jg''(J)$ is negative for $J > 0$.

4.2. Boundary Conditions

We seek growth-induced cavitation without loading, so we assume zero radial force at both the inner and outer radii of the cavitated configuration. With the Varga strain energy density, the left-hand side of Equation (2.13) takes the form

$$\lambda_3\overline{\sigma}_{11} = \lambda_3\mu\left(\frac{1}{\lambda_2\lambda_3} - g'(J)\right) = \mu\left(\frac{1}{\lambda_2} - J\left(g'(J)\right)^2\right), \tag{4.8}$$

where the last equality holds because of the plane-stress condition, Equation (4.3). In the presence of a cavity, there is no reason to assume that the principal stretches are well-behaved near the surface of the cavity, which is reached in the $R \to 0$ limit. We consider the possible behaviors of J in this limit.

4.2.1. $\lim_{\mathbf{R}\to\mathbf{0}}\mathbf{J}(\mathbf{R}) \in (\mathbf{0}, \infty)$

In the case of a nonzero finite limit, $\lim_{R\to 0} J(R) = J_0$, we have

$$\lim_{R\to 0}\lambda_3\overline{\sigma}_{11} = \lim_{R\to 0}\mu\left(\frac{1}{\lambda_2} - J\left(g'(J)\right)^2\right) = -\mu J_0\left(g'(J_0)\right)^2, \tag{4.9}$$

where $\lambda_2^{-1} = \gamma_2 R/r \to 0$ as $R \to 0$. Since we assume that $g'(J)$ is positive for $J > 0$, this leaves us with a nonzero force at the inner radius of the deformed configuration, and this case is ruled out.

4.2.2. $\lim_{R\to 0} J(R) = 0$

We divide this case into three distinct sub-cases, depending on the behavior of $g'(J)$ as $J \to 0$.

Sub-Case I: $\mathbf{g'(0) = 0}$ Suppose first that $g'(0) = 0$. Since we assume g to be twice continuously differentiable for $J > 0$, we have

$$g'(J) = \int_0^J g''(x)\mathrm{d}x < 0 \tag{4.10}$$

because $g''(J) < 0$ for $J > 0$. But this contradicts our assumption that $g'(J) > 0$ for $J > 0$.

Sub-Case II: $\mathbf{g'(0) \in (0, \infty)}$ Now suppose that $g'(0) \in (0, \infty)$. Then $J \to 0$ and $J\left(g'(J)\right)^2 \to 0$ as $R \to 0$. Recall that

$$J' = \frac{\gamma_2 - \gamma_1}{rg'(J)\left(g'(J) + 2Jg''(J)\right)}, \quad \text{while} \quad \frac{\mathrm{d}}{\mathrm{d}R} J\left(g'(J)\right)^2 = \frac{\gamma_2 - \gamma_1}{r}.$$

Since $J(0) = 0$ and since $J(R) > 0$ for $R > 0$, J' must be nonnegative at $R = 0$. Since $g'(J) > 0$ and $g'(J) + 2Jg''(J) < 0$ for $J > 0$ (and thus for $R > 0$), we have

$$\operatorname{sign}\left(J'\right) = \frac{\operatorname{sign}\left(\gamma_2 - \gamma_1\right)}{\operatorname{sign}\left(rg'(J)\right)\operatorname{sign}\left(g'(J) + 2Jg''(J)\right)} = \operatorname{sign}\left(\gamma_1 - \gamma_2\right). \tag{4.11}$$

Thus we require $\gamma_1 > \gamma_2$.

But $J\left(g'(J)\right)^2$ is also zero at $R = 0$ and must also be positive for $R > 0$. Now note that

$$\operatorname{sign}\left(\frac{\mathrm{d}}{\mathrm{d}R} J\left(g'(J)\right)^2\right) = \frac{\operatorname{sign}\left(\gamma_2 - \gamma_1\right)}{\operatorname{sign}(r)} = \operatorname{sign}\left(\gamma_2 - \gamma_1\right). \tag{4.12}$$

For positivity of $J\left(g'(J)\right)^2$, we require $\gamma_2 > \gamma_1$, which contradicts the last result. Thus we eliminate the case in which $g'(0) = 0$.

Sub-Case III: $\mathbf{\lim_{J\to 0} g'(J) = \infty}$ Finally we consider $\lim_{J\to 0} g'(J) = \infty$. Since

$$\frac{\mathrm{d}}{\mathrm{d}R} J\left(g'(J)\right)^2 = \frac{\gamma_2 - \gamma_1}{r}$$

and since the right-hand side of this equation converges to a finite value as $R \to 0$, $J\left(g'(J)\right)^2$ also converges as $R \to 0$. As argued above, since $J(0) = 0$ and since $J(R)$ must be positive for $R > 0$, we require $\gamma_1 > \gamma_2$. As a result, the derivative of $J\,(g'(J))^2$ is negative at $R = 0$, so $J\,(g'(J))^2$, must be positive at $R = 0$. Otherwise, $J\,(g'(J))^2$, would be negative for small positive values of R.

Let $\lim_{R\to 0} J\,(g'(J))^2 = \beta > 0$. Then

$$J(R)\left(g'(J(R))\right)^2 - \beta = \int_0^R \frac{\gamma_2 - \gamma_1}{r(s)}\mathrm{d}s < 0. \tag{4.13}$$

This implies

$$0 < \beta - J(R)\left(g'(J(R))\right)^2 = (\gamma_1 - \gamma_2)\int_0^R \frac{\mathrm{d}s}{r(s)} < \frac{(\gamma_1 - \gamma_2)R}{r(0)}, \tag{4.14}$$

as $r(0) < r(R)$ for $R > 0$. Hence $J\,(g'(J))^2 = \beta + \mathcal{O}(R)$ as $R \to 0$. The radial force at $r(0)$ is then proportional to

$$\lim_{R\to 0} \lambda_3\overline{\sigma}_{11} = \lim_{R\to 0} \mu\left(\frac{1}{\lambda_2} - J\left(g'(J)\right)^2\right) = -\mu\beta.$$

Because of this nonzero radial force at $R = 0$, we rule out this case.

4.2.3. $\mathbf{\lim_{R\to 0} J\,(R) = \infty}$

The only possibility that remains is the divergence of J as $R \to 0$. We consider two distinct limiting behaviors of $g'(J)$ as $J \to \infty$.

Sub-Case I: $\mathbf{\lim_{J\to\infty} g'(J) > 0}$ In this case, proceeding as above shows that

$$\lim_{R\to 0} \lambda_3\overline{\sigma}_{11} = \mu\left(\lim_{R\to 0}\frac{1}{\lambda_2} - \lim_{R\to 0} J\left(g'(J)\right)^2\right) = -\infty. \tag{4.15}$$

This precludes the possibility that $\lim_{J\to\infty} g'(J) > 0$.

Sub-Case II: $\mathbf{\lim_{J\to\infty} g'(J) = 0}$ In this category we have found an example of growth-induced cavitation that is sustained with zero radial traction on the cavity's surface. This example is presented in the next section.

4.3. A Necessary Condition

Before we explore this very specific example, we note a physically meaningful condition that is necessary for growth-induced cavitation. Since $J \to \infty$ as $R \to 0$ and since J must be finite within the body, we must have $J' \to -\infty$ as $R \to 0$. However, the form of J' (Equation (4.6)) and the restrictions on $g'(J)$ and $g'(J) + 2Jg''(J)$ ensure that J' is negative throughout the body. And since

$$\operatorname{sign}(J') = \operatorname{sign}\left(\gamma_1 - \gamma_2\right),$$

cavitation with zero radial traction is possible only if $\gamma_2 > \gamma_1$.

4.4. Constructing an Appropriate $\mathbf{g'(J)}$

The following class of functions satisfies all the requirements so far imposed on $g(J)$:

$$g(J) = A\left(-\frac{1}{\alpha}J^{-\alpha} + 3 + \frac{1}{\alpha}\right) + (1-A)\left(2J^{1/2}+1\right),$$

where $\alpha > 0$ and $A > (6\alpha+3)^{-1}$.

However, even this small class must be reduced before we have a physically acceptable g. Since the thickness of the membrane is proportional to λ_3, λ_3 must not diverge as $R \to 0$. The plane-stress condition requires $\lambda_3 = Jg'(J)$ (Equation (4.3)), which in this case amounts to

$$\lambda_3 = AJ^{-\alpha} + (1-A)J^{1/2}.$$

Since we now assume $J \to \infty$ as $R \to 0$, this would imply $\lambda_3 \to \infty$ as $R \to 0$. Hence we set $A = 1$:

$$\begin{aligned} g(J) &= -\frac{1}{\alpha}J^{-\alpha} + 3 + \frac{1}{\alpha}, && (4.16)\\ g'(J) &= J^{-\alpha-1}, && (4.17)\\ g'(J) + 2Jg''(J) &= -(2\alpha+1)J^{-\alpha-1}. && (4.18) \end{aligned}$$

Equations (4.6)–(4.7) now take the form

$$J' = \frac{\left(\gamma_1 - \gamma_2\right) J^{2\alpha+2}}{(2\alpha+1)r}, \tag{4.19}$$

$$r' = \frac{\gamma_1\gamma_2 R J^{\alpha+1}}{r}. \tag{4.20}$$

4.5. Converting to an Autonomous System

Due to the explicit presence of R in Equation (4.20), Equations (4.19)–(4.20) do not define an autonomous system. To produce an equivalent autonomous system, set $\tau = -\ln(R/B)$ for some $B > 0$, and set $q = r/R$.

$$\frac{\mathrm{d}J}{\mathrm{d}\tau} = \left(\frac{\gamma_2 - \gamma_1}{2\alpha+1}\right) J^{2\alpha+2} q, \tag{4.21}$$

$$\frac{dq}{d\tau} = q - \gamma_1 \gamma_2 J^{\alpha+1} q^{-1}, \tag{4.22}$$

and the behavior as $R \to 0$ now corresponds to the behavior of the two dependent variables as the new "time" $\tau \to \infty$

4.6. Converting to a Lotka–Volterra System

Demonstrating the existence of a solution with the desired asymptotic behavior is easier if the autonomous system above is now converted to a Lotka–Volterra system. Setting

$$Z_1 = J^{2\alpha+1} q^{-1}, \tag{4.23}$$

$$Z_2 = J^{\alpha+1} q^{-2}, \tag{4.24}$$

results in

$$\frac{dZ_1}{d\tau} = -Z_1 + (\gamma_2 - \gamma_1) Z_1^2 + \gamma_1 \gamma_2 Z_1 Z_2, \tag{4.25}$$

$$\frac{dZ_2}{d\tau} = -2Z_2 + 2\gamma_1 \gamma_2 Z_2^2 + \frac{(\gamma_2 - \gamma_1)(\alpha + 1)}{2\alpha + 1} Z_1 Z_2 \tag{4.26}$$

4.7. Asymptotics of the Lotka–Volterra System

We have established that in a configuration with a cavity, both J and q diverge as $R \to 0$. Hence as $\tau \to \infty$,

$$\frac{Z_2}{Z_1} = \frac{J^{\alpha+1} q^{-2}}{J^{2\alpha+1} q^{-1}} = J^{-\alpha} q^{-1} \to 0. \tag{4.27}$$

Any orbit of the Lotka–Volterra system for which Z_2/Z_1 diverges or converges to a positive constant, does not correspond to a cavitated configuration.

We introduce one more useful fact before addressing specific orbits. The definition of q and Equation (4.22) reveal that

$$\frac{dr}{d\tau} = \frac{d}{d\tau}\left(qBe^{-\tau}\right) = q'Be^{-\tau} - qBe^{-\tau} = -\gamma_1 \gamma_2 J^{\alpha+1} q^{-1} Be^{-\tau}. \tag{4.28}$$

Combining this with the definition $q = r/R$ and Equation (4.24) shows that

$$\frac{d}{d\tau} \ln r = -\gamma_1 \gamma_2 Z_2. \tag{4.29}$$

Now we may consider the growth or decay of Z_2 to determine whether $\ln r$ converges as $R \to 0$ (as $\tau \to \infty$).

4.7.1. Unbounded orbits

We consider only those unbounded orbits on which $Z_1 \gg Z_2$ asymptotically. It is evident from Equation (4.26) that if the orbit does not converge to a fixed point and $Z_1 \gg Z_2$, then Z_2 does not decay rapidly to zero as $\tau \to \infty$. Hence,

$$\lim_{\tau \to \infty} \ln r = -\infty, \tag{4.30}$$

and $\lim_{R\to 0} r = 0$ on this orbit. No unbounded orbit corresponds to a cavitated configuration.

The system defined by Equations (4.25)–(4.26) has three fixed points. The coordinates, linearizations of the equations, and eigenvalues of these fixed points are listed in the table below.

Coordinates (z_1, z_2)	Linearization $D\mathbf{f}(z_1, z_2)$	Eigenvalues
$(0, 0)$	$\begin{pmatrix} -1 & 0 \\ 0 & -2 \end{pmatrix}$	$-1, -2$
$\left(0, \frac{1}{\gamma_1\gamma_2}\right)$	$\begin{pmatrix} 0 & 0 \\ \frac{(\gamma_2-\gamma_1)(\alpha+1)}{\gamma_1\gamma_2(2\alpha+1)} & 2 \end{pmatrix}$	$0, 2$
$\left(\frac{1}{\gamma_2-\gamma_1}, 0\right)$	$\begin{pmatrix} 1 & \frac{\gamma_1\gamma_2}{\gamma_2-\gamma_1} \\ 0 & -\left(\frac{3\alpha+1}{2\alpha+1}\right) \end{pmatrix}$	$1, -\left(\frac{3\alpha+1}{2\alpha+1}\right)$

4.7.2. Fixed point $(\mathbf{0}, \mathbf{0})$

The eigenvalues of $D\mathbf{f}(0, 0)$ indicate that $(0, 0)$ is a sink. We consider orbits attracted to $(0, 0)$. Note that by Equations (4.23)–(4.24),

$$J^{3\alpha+1} = \frac{Z_1^2}{Z_2} \tag{4.31}$$

so that by Equations (4.25)–(4.26),

$$\frac{\mathrm{d}}{\mathrm{d}\tau} J^{3\alpha+1} = \frac{(\gamma_2 - \gamma_1)(3\alpha + 1)}{2\alpha + 1} Z_1 J^{3\alpha+1}, \tag{4.32}$$

or

$$\frac{\mathrm{d}}{\mathrm{d}\tau} \ln\left(J^{3\alpha+1}\right) = \frac{(\gamma_2 - \gamma_1)(3\alpha + 1)}{2\alpha + 1} Z_1, \tag{4.33}$$

or, even more directly,

$$\frac{\mathrm{d}}{\mathrm{d}\tau}\ln J = \left(\frac{\gamma_2-\gamma_1}{2\alpha+1}\right) Z_1. \tag{4.34}$$

By Equation (4.25), given any $\delta \in (0,1)$, for (Z_1, Z_2) in the first quadrant and close enough to $(0,0)$,

$$\frac{\mathrm{d}Z_1}{\mathrm{d}\tau} < (-1+\delta)\, Z_1. \tag{4.35}$$

For large-enough $\tau_0 < \tau$, then,

$$Z_1(\tau) < Z_1(\tau_0) e^{(-1+\delta)(\tau-\tau_0)}. \tag{4.36}$$

Integrating Equation (4.34) yields

$$\begin{aligned} \ln\left(\frac{J(\tau)}{J(\tau_0)}\right) &= \left(\frac{\gamma_2-\gamma_1}{2\alpha+1}\right)\int_{\tau_0}^{\tau} Z_1(s)\mathrm{d}s \\ &< \left(\frac{\gamma_2-\gamma_1}{2\alpha+1}\right) Z_1(\tau_0)\int_{\tau_0}^{\tau} \mathrm{e}^{(-1+\delta)(s-\tau_0)}\mathrm{d}s \\ &= \left(\frac{\gamma_2-\gamma_1}{2\alpha+1}\right)\frac{Z_1(\tau_0)}{1-\delta}\left(1-\mathrm{e}^{(-1+\delta)(\tau-\tau_0)}\right) \end{aligned} \tag{4.37}$$

Taking the $\tau \to \infty$ limit of Equation (4.37) shows

$$\lim_{\tau\to\infty} \ln\left(\frac{J(\tau)}{J(\tau_0)}\right) \leq \left(\frac{\gamma_2-\gamma_1}{2\alpha+1}\right)\frac{Z_1(\tau_0)}{1-\delta} < \infty. \tag{4.38}$$

Equation (4.38) reveals that on an orbit attracted to the fixed point $(0,0)$, J does not diverge as $\tau \to \infty$. Such orbits correspond to configurations with nonzero radial traction at the surface of the cavity.

4.7.3. Fixed point $(0, \gamma_1^{-1}\gamma_2^{-1})$

The presence of one positive eigenvalue and one zero eigenvalue of $D\mathbf{f}(\gamma_1^{-1}\gamma_2^{-1}, 0)$ ensures the existence of a one-dimensional center manifold for this fixed point; see, e.g., [40]. At the fixed point, the center manifold is tangent to the 0-eigenspace of $D\mathbf{f}(\gamma_1^{-1}\gamma_2^{-1}, 0)$. If any orbit approaches this fixed point, it lies on the center manifold.

Suppose that there is an orbit that approaches this fixed point as $\tau \to \infty$. Since Z_2 converges to a positive constant, $J^{\alpha+1}$ and q^2 must have the same asymptotic growth rates. Since $J^{\alpha+1}$ diverges, q^2 grows at the same rate. But then

$$Z_1 = \frac{J^{2\alpha+1}}{q} = \frac{\left(J^{\alpha+1}\right)^{(2\alpha+1)/(\alpha+1)}}{\left(q^2\right)^{1/2}} > \frac{J^{\alpha+1}}{q^2} \to \left(\gamma_1\gamma_2\right)^{-1}.$$

However, $Z_1 \to 0$ as the orbit approaches this fixed point, contradicting the above inequality. Hence the orbit approaching this fixed point (along the center manifold) as $\tau \to \infty$ does not correspond to a cavitated configuration.

4.7.4. Fixed point $(\gamma_2-\gamma_1)^{-1}, 0)$

The linearization at this fixed point has one positive and one negative eigenvalue, so this fixed point has a one-dimensional stable manifold; see [40]. We consider the orbit that approaches the fixed point along the stable manifold from the first quadrant. Z_1 converges to $(\gamma_2-\gamma_2)^{-1}$, while Z_2 converges to 0. We will now show that the stable manifold corresponds to a function $r(R)$ that converges to a positive constant as $R \to 0$ (i.e. as $\tau \to \infty$).

Recall from Equation (4.29) that

$$\frac{\mathrm{d}}{\mathrm{d}\tau} \ln r = -\gamma_1 \gamma_2 Z_2. \tag{4.39}$$

$Z_2 \to 0$ on the stable manifold, and we will show that $Z_2 \to 0$ fast enough that $\lim_{\tau\to\infty} \ln r > -\infty$.

Since $Z_2 \to 0$ and $Z_1 \to (\gamma_2 - \gamma_1)^{-1}$ on the stable manifold, for small $\delta > 0$ and (Z_1, Z_2) close enough to $\left((\gamma_2 - \gamma_1)^{-1}, 0\right)$,

$$\begin{aligned} \frac{\mathrm{d}Z_2}{\mathrm{d}\tau} &< \left(-2 + \delta + \frac{(\gamma_2 - \gamma_1)(\alpha + 1)}{2\alpha + 1}\left(\frac{1}{\gamma_2 - \gamma_1} + \delta\right)\right) Z_2 \\ &= \left(-\left(\frac{3\alpha + 1}{2\alpha + 1}\right) + \left(1 + \frac{(\gamma_2 - \gamma_1)(\alpha + 1)}{2\alpha + 1}\right)\delta\right) Z_2, \end{aligned}$$

so that for $\tau > \tau_0$,

$$\frac{Z_2(\tau)}{Z_2(\tau_0)} < \exp\left(\left\{-\left(\frac{3\alpha + 1}{2\alpha + 1}\right) + \left(1 + \frac{(\gamma_2 - \gamma_1)(\alpha + 1)}{2\alpha + 1}\right)\delta\right\}(\tau - \tau_0)\right). \tag{4.40}$$

If δ is chosen small enough and τ_0 is chosen large enough, then from Equations (4.39) and (4.40) for $\tau > \tau_0$ we have

$$-\gamma_1\gamma_2 Z_2(\tau_0)\mathrm{e}^{-\eta(\tau-\tau_0)} < \frac{\mathrm{d}}{\mathrm{d}\tau} \ln r < 0, \tag{4.41}$$

where

$$\eta = \left(\frac{3\alpha + 1}{2\alpha + 1}\right) - \left(1 + \frac{(\gamma_2 - \gamma_1)(\alpha + 1)}{2\alpha + 1}\right)\delta > 0.$$

Integration yields

$$\frac{\gamma_1\gamma_2 Z_2(\tau_0)}{\eta}\left(\mathrm{e}^{-\eta\tau} - \mathrm{e}^{-\eta\tau_0}\right) < \ln\left(\frac{r(\tau)}{r(\tau_0)}\right) < 0, \tag{4.42}$$

so that

$$\lim_{\tau\to\infty} \ln r(\tau) \geq \ln r(\tau_0) - \frac{\gamma_1\gamma_2 Z_2(\tau_0)}{\eta}\mathrm{e}^{-\eta\tau_0} > -\infty. \tag{4.43}$$

Hence $r(R)$ converges to a positive constant as $R \to 0$.

It can be shown that each orbit attracted to the fixed point (0, 0) also has a radius converging to a positive number as $\tau \to \infty$ ($R \to 0$). However, such orbits have been discounted because J does not diverge as $\tau \to \infty$. We now establish that J does diverge on the stable manifold of $\left((\gamma_2 - \gamma_1)^{-1}, 0\right)$.

It can be shown from Equations (4.23)–(4.24) that

$$J^{3\alpha+1} = \frac{Z_1^2}{Z_2}. \tag{4.44}$$

On the stable manifold of $\left((\gamma_2 - \gamma_1)^{-1}, 0\right)$, $Z_1 \to (\gamma_2 - \gamma_1)^{-1} > 0$ and $Z_2 \to 0$ as $\tau \to \infty$. Hence J diverges as $\tau \to \infty$, and the radial traction at the surface of the cavity is zero.

We have established the existence of a solution $R \mapsto r(R)$ that converges to a positive constant as $R \to 0$ and has zero radial stress in the same limit. Now we must demonstrate that this solution has zero radial stress at some positive value of R. The corresponding value of r is the outer radius of a cavitated configuration with zero radial stress at the inner and outer radii.

4.8. Boundary Condition at Outer Radius

From Equations (4.8) and (4.17) we see that

$$\lambda_3\overline{\sigma}_{11} = \mu\left(\frac{\gamma_2}{q} - J^{-(2\alpha+1))}\right). \tag{4.45}$$

For $R > 0$ both J and q are positive and finite, so the zero-radial force condition implies $q/\gamma_2 = J^{2\alpha+1}$, or

$$Z_1 = \frac{J^{2\alpha+1}}{q} = \frac{1}{\gamma_2}. \tag{4.46}$$

If the stable manifold of the fixed point $((\gamma_2 - \gamma_1)^{-1}, 0)$ intersects the line $Z_1 = \gamma_2^{-1}$ in the (Z_1, Z_2)-plane, then the portion of the orbit from the fixed point to this line corresponds to a cavitated configuration that has zero radial traction applied at its inner and outer radii.

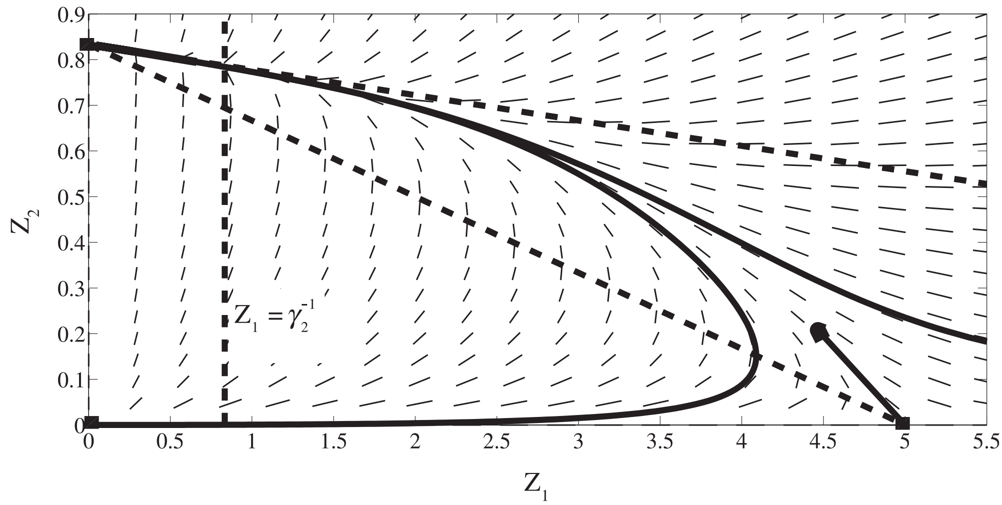

Figure 1. Phase portrait for $\gamma_1 = 1.0$, $\gamma_2 = 1.2$, $\alpha = 1$: Each fixed point is marked by a black square. The vertical dashed line is $Z_1 = \gamma_2^{-1}$. The solid lines are two orbits of the system. Between the slanted dashed lines, $\mathrm{d}Z_1/\mathrm{d}\tau > 0$ and $\mathrm{d}Z_2/\mathrm{d}\tau < 0$. The arrow emanating from the fixed point $\left((\gamma_2-\gamma_1)^{-1}, 0\right) = (5, 0)$ points along the stable eigenspace at this point. The stable manifold at this fixed point is asymptotically tangent to this line.

$$\frac{\mathrm{d}Z_1}{\mathrm{d}\tau} = 0 \quad \text{for} \quad Z_2 = -\left(\frac{\gamma_2-\gamma_1}{\gamma_2\gamma_1}\right) Z_1 + \frac{1}{\gamma_1\gamma_2}, \tag{4.47}$$

$$\frac{\mathrm{d}Z_1}{\mathrm{d}\tau} = 0 \quad \text{for} \quad Z_2 = -\left(\frac{\alpha+1}{4\alpha+2}\right)\left(\frac{\gamma_2-\gamma_1}{\gamma_2\gamma_1}\right) Z_1 + \frac{1}{\gamma_1\gamma_2}. \tag{4.48}$$

The slope of line in Equation (4.47) is more severe than that of the line in Equation (4.48), and these lines intersect at the fixed point $(0, \gamma_1^{-1}\gamma_2^{-1})$. It can be seen from Equations (4.25)–(4.26) that $dZ_1/d\tau > 0$ and $\mathrm{d}Z_2/\mathrm{d}\tau < 0$ between these lines in the first quadrant of the plane. Hence any orbit that is in this region for some τ_0 is trapped in this region for $\tau \leq \tau_0$ and approaches the fixed point $(0, \gamma_1^{-1}, \gamma_2^{-1})$ as $\tau \to -\infty$.

The stable manifold of the fixed point $\left((\gamma_2-\gamma_1)^{-1}, 0\right)$ is asymptotically tangent to the "stable eigenspace" at this fixed point. The linearization of Equations (4.25)–(4.26) at this fixed point reveals that

$$\begin{pmatrix} -(2\alpha+1)\gamma_2\gamma_2 \\ (5\alpha+1)(\gamma_2-\gamma_1) \end{pmatrix} \tag{4.49}$$

is a representative vector from this eigenspace. When attached to the fixed point $\left((\gamma_2-\gamma_1)^{-1}, 0\right)$, this vector points into the region between the lines described in Equations (4.47)–(4.48); see Figure 1. The stable manifold lies between the lines for all τ and

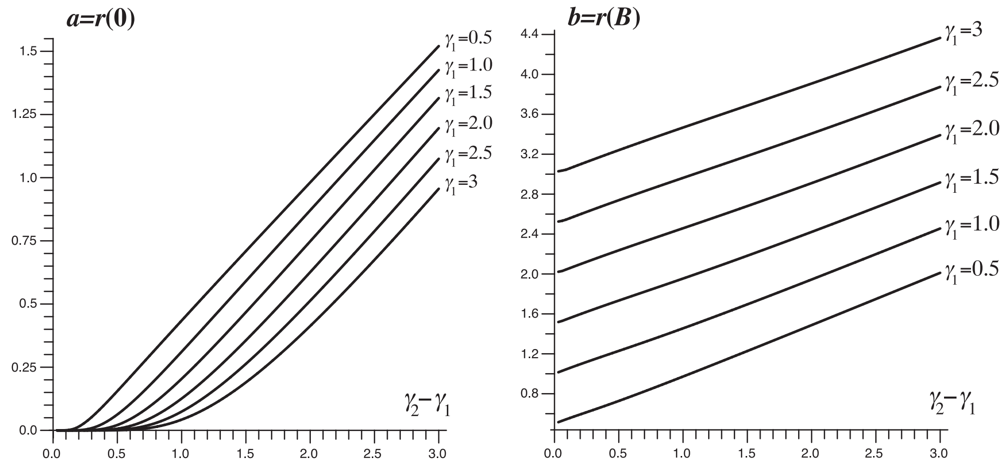

Figure 2. Cavity radius $a = r(0)$ and outer radius $b = r(B)$ as functions of $\gamma_2 - \gamma_1$ for various values of γ_1.

thus intersects the line $Z_1 = \gamma_2^{-1}$. The orbit of interest to us approaches the fixed point $\left((\gamma_2 - \gamma_1)^{-1}, 0\right)$ as $\tau \to \infty$ and the fixed point $(0, \gamma_1^{-1}\gamma_2^{-1})$ as $\tau \to -\infty$.

4.9. Numerical Construction of Solutions

To compute the radius of a cavity numerically, a point on the stable eigenspace attached to the fixed point $\left((\gamma_2 - \gamma_1)^{-1}, 0\right)$ was chosen very close to the fixed point. With this point as initial condition, the system Equations (4.25)–(4.26) was integrated numerically backward in τ until the numerical orbit reached the line $Z_1 = \gamma_2^{-1}$. This enforced a condition of zero radial traction at the maximum value of R, i.e. at the outer perimeter of the membrane. The elapsed τ was then used to compute

$$r = qR = \left(\frac{Z_1^{\alpha+1}}{Z_2^{2\alpha+1}}\right)^{1/(3\alpha+1)} B\mathrm{e}^{-\tau}. \tag{4.50}$$

The coordinates of the initial condition provided the values of Z_1 and Z_2, and B was set to 1. The results showing $\lim_{R\to 0} r(R)$ as a function of γ_2 are shown for various values of γ_1 in Figure 2.

The same numerical integration was used to compute the outer radius of the membrane after deformation. In Equation (4.50), τ is set to 0, B is set to 1, Z_1 is set to γ_2^{-1}, and the value of Z_2 is that found by numerical integration to the point where the orbit crosses the line $Z_1 = \gamma_2^{-1}$.

On each curve the radius of the cavity increases with $\gamma_2 - \gamma_1$. However, the curves describing the cavity's radius are not mere translates of one another; the growth with $\gamma_2 - \gamma_1$ is slower for larger values of γ_1. On the other hand, the curves showing the outer radius of the membrane do appear to be parallel.

5. CONCLUSION

In this paper, we considered the effect of anisotropic homogeneous growth in the cavitation of compressible elastic membranes. While the neo-Hookean membrane does not support cavitated solutions, the Varga membrane can admit cavitated solutions. Moreover, when the azimuthal growth(characterized by the parameter γ_2) is larger than the radial growth, the membrane spontaneously cavitates, that is, without external traction.

The analysis relies on a transformation of both dependent and independent variables to reduce the governing equations to a system of two autonomous ordinary differential equations that can be studied with the classical tools of dynamical systems theory. In particular the proof of the existence of cavitated solution reduces to showing the existence of a particular solution curve in the phase plane connecting a fixed point to a particular line. Further, the dynamical systems analogy can be used to compute the opening of the cavity as the parameters are varied. This analogy can be further extended to obtain estimates and bounds on the solution, if needed.

Acknowledgments. The authors would like to thank Professor S. Venkataramani for helpful discussions. This material is based in part upon work supported by the National Science Foundation under grant No. DMS-0604704 (A. G. and M. T.).

APPENDIX

The first step is to combine Equations (2.10) and (4.2).

$$\frac{\mu}{\gamma_1\lambda_1\lambda_3}\frac{\mathrm{d}}{\mathrm{d}R}\left(\lambda_3\left(\frac{1}{\lambda_2\lambda_3}-g'(J)\right)\right)+\frac{\mu}{r}\left(\frac{1}{\lambda_2\lambda_3}-\frac{1}{\lambda_1\lambda_3}\right)=0,$$

which simplifies to

$$\frac{1}{\gamma_1\lambda_1\lambda_3}\frac{\mathrm{d}}{\mathrm{d}R}\left(\frac{1}{\lambda_2}-\lambda_3 g'(J)\right)+\frac{1}{r}\left(\frac{1}{\lambda_2\lambda_3}-\frac{1}{\lambda_1\lambda_3}\right)=0. \tag{A.1}$$

Note that

$$\frac{\mathrm{d}}{\mathrm{d}R}\lambda_2^{-1}=\frac{\mathrm{d}}{\mathrm{d}R}\left(\frac{\gamma_2 R}{r}\right)=\gamma_2\left(\frac{1}{r}-\frac{Rr'}{r^2}\right)=\frac{\gamma_2}{r}\left(1-\frac{\gamma_1\lambda_1}{\gamma_2\lambda_2}\right).$$

When this is plugged into Equation (A.1) we find

$$\frac{1}{\gamma_1\lambda_1\lambda_3}\left(\frac{\gamma_2}{r}\left(1-\frac{\gamma_1\lambda_1}{\gamma_2\lambda_2}\right)-\frac{\mathrm{d}}{\mathrm{d}R}\left(\lambda_3 g'(J)\right)\right)+\frac{1}{r}\left(\frac{1}{\lambda_2\lambda_3}-\frac{1}{\lambda_1\lambda_3}\right)=0.$$

$$\frac{\mathrm{d}}{\mathrm{d}R}\left(\lambda_3 g'(J)\right)=\frac{\gamma_2}{r}\left(1-\frac{\gamma_1\lambda_1}{\gamma_2\lambda_2}\right)+\frac{\gamma_1\lambda_1\lambda_3}{r}\left(\frac{1}{\lambda_2\lambda_3}-\frac{1}{\lambda_1\lambda_3}\right)$$

$$= \frac{\gamma_2}{r} - \frac{\gamma_1\lambda_1}{\lambda_2 r} + \frac{\gamma_1\lambda_1}{\lambda_2 r} - \frac{\gamma_1}{r}$$

$$= \frac{\gamma_2 - \gamma_1}{r}$$

The plane stress condition, Equation (4.3), allows us to eliminate λ_3:

$$\frac{\mathrm{d}}{\mathrm{d}R}\left(J\left(g'(J)\right)^2\right) = \frac{\gamma_2 - \gamma_1}{r}. \tag{A.2}$$

If J' is the derivative of J with respect to R, then we have

$$J'\left(g'(J)\right)^2 + 2Jg'(J)g''(J)J' = \frac{\gamma_2 - \gamma_1}{r},$$

or

$$J' = \frac{\gamma_2 - \gamma_1}{rg'(J)\left(g'(J) + 2Jg''(J)\right)},$$

which is Equation (4.7).

To derive Equation (4.6) we adapt Equation (2.9) with the definition $J = \lambda_1\lambda_2\lambda_3$.

$$\frac{\mathrm{d}r}{\mathrm{d}R} = \gamma_1\lambda_1 = \gamma_1\frac{J}{\lambda_2\lambda_3} = \gamma_1\frac{J}{(r/\gamma_2 R)Jg'(J)} = \frac{\gamma_1\gamma_2 R}{rg'(J)} \tag{A.3}$$

REFERENCES

[1] R. Skalak, Zargaryan, S., Jain, R. K., Netti, P. A. and Hoger, A. Compatibility and the genesis of residual stress by volumetric growth. *Journal of Mathematical Biology*, 34, 889–914 (1996).

[2] Fung, Y. C. *Biomechanics: Mechanical Properties of Living Tissues*, Springer, New York, 1993.

[3] Humphrey, J. D. *Cardiovascular Solid Mechanics. Cells, Tissues, and Organs*, Springer, New York, 2002.

[4] Ben Amar, M. and Goriely, A. Growth and instability in soft tissues. *Journal of Mechanics and Physics of Solids,* 53, 2284–2319 (2005).

[5] Goriely, A. and Ben Amar, M. Differential growth and instability in elastic shells. *Physics Review Letters*, 94, 198103 (2005).

[6] Gent, A. N. and Lindley, P. B. *Internal rupture of bonded rubber cylinders in tension. Proceedings of the Royal Society of London, Series A, Mathematical and Physical Sciences*, 249, 195–205 (1959).

[7] Ball, J. M. Discontinuous equilibrium solutions and cavitation in nonlinear elasticity. *Philosophical Transactions of the Royal Society of London, Series A, Mathematical and Physical Sciences*, 306, 557–611 (1982).

[8] Polignone, D. A. and Horgan, C. O. Cavitation for incompressible anisotropic nonlinearly elastic spheres. *Journal of Elasticity*, 33, 27–65 (1993).

[9] Horgan, C. O. and Polignone, D. A. Cavitation in nonlinearly elastic solids: A review. *Applied Mechanics Review*, 48, 471–485 (1995).

[10] Sivaloganathan, J. On cavitation and degenerate cavitation under internal hydrostatic pressure. *Proceedings of the Royal Society A: Mathematical, Physical and Engineering Sciences*, 455, 3645–3664 (1999).

[11] Horgan, C. O. Equilibrium solutions for compressible nonlinearly elastic materials, in *Nonlinear Elasticity: Theory and Applications*, ed. R. W. Ogden and Y. Fu, London Mathematical Society Lecture Notes, Vol 283, pp. 135—159, Cambridge University Press, 2001.

[12] Sivaloganathan, J. and Spector, S. J. On cavitation, configurational forces and implications for fracture in a nonlinearly elastic material. *Journal of Elasticity*, 67, 25–49 (2002).

[13] Pericak-Spector, K. A., Sivaloganathan, J. and Spector, S. J. An explicit radial cavitation solution in nonlinear elasticity. *Mathematics and Mechanics of Solids*, 7, 87 (2002).

[14] Pence, T. J. and Tsai, H. On the cavitation of a swollen compressible sphere in finite elasticity. *International Journal of Non-Linear Mechanics*, 40, 307–321, 2005.

[15] Pence, T. J. and Tsai, H. Swelling induced cavitation of elastic spheres. *Mathematics and Mechanics of Solids*, 11, 527 (2006).

[16] Tvergaard, V. Effect of void size difference on growth and cavitation instabilities. *Journal of the Mechanics and Physics of Solids*, 44, 1237–1253 (1996).

[17] Fond, C. Cavitation criterion for rubber materials: a review of void-growth models. *Journal of Polymer Science B: Polymer Physics*, 39, 2081–2096 (2001).

[18] Dollhofer, J., Chiche, A., Muralidharan, V., Creton, C. and Hui, C. Y. Surface energy effects for cavity growth and nucleation in an incompressible neo-Hookean material—modeling and experiment. *International Journal of Solids and Structures*, 41, 6111–6127 (2004).

[19] Haughton, D. M. *Nonlinear Elasticity: Theory and Applications*, chapter Elastic membranes, pp. 233–267, Cambridge University Press, Cambridge, 2001.

[20] Haughton, D. M. On non-existence of cavitation in incompressible elastic membranes. *Quarterly Journal of Mechanics and Applied Mathematics*, 39, 289–296 (1986).

[21] Steigmann, D. J. Cavitation in elastic membranes—an example. *Journal of Elasticity*, 28, 277–287 (1992).

[22] Nadler, B. and Steigmann, D. J. Modeling the indentation, penetration and cavitation of elastic membranes. *Journal of the Mechanics and Physics of Solids*, 54, 2005–2029 (2006).

[23] Rodriguez, E. K., Hoger, A. and McCulloch, A. Stress-dependent finite growth in soft elastic tissue. *Journal of Biomechanics*, 27, 455–467 (1994).

[24] Lin, L. E. and Taber, L. A model for stress-induced growth in the developing heart. *Journal of Biomechanical Engineering*, 117, 343–349 (1995).

[25] Taber, L. A. Biomechanics of growth, remodeling and morphogenesis. *Applied Mechanics Review*, 48, 487–545 (1995).

[26] Taber, L. A. and Eggers, D. W. Theoretical study of stress-modulated growth in the aorta. *Journal of Theoretical Biology*, 180, 343–357 (1996).

[27] Taber, L. A. Biomechanical growth laws for muscle tissues. *Journal of Theoretical Biology*, 193, 201–213 (1998).

[28] Taber, L. A. A model of aortic growth based on fluid shear and fiber stresses. *Journal of Biomechanical Engineering*, 120, 348–354 (1998).

[29] Taber, L. A. and Humphrey, J. D. Stress-modulated growth, residual stress, and vascular heterogeneity. *Journal of Biomechanical Engineering*, 123, 528–535 (2001).

[30] Klisch, S. M., Chen, S. S., Sah, R. S. and Hoger, A. A growth mixture theory for cartilage with application to growth-related experiments on cartilage explants. *Journal of Biomechanical Engineering*, 125, 169–179 (2003).

[31] Humphrey, J. D. Continuum biomechanics of soft biological tissues. *Proceedings of the Royal Society of London A,* 459, 3–46 (2003).

[32] Cowin, S. C. Tissue growth and remodeling. *Annual Reviews in Biomedical Engineering*, 6, 77–107 (2004).

[33] Ambrosi, D. and Mollica, F. The role of stress in the growth of a multicell spheroid. *Journal of Mathematical Biology*, 48, 477–499 (2004).

[34] Chen, Y. and Hoger, A. Constitutive functions of elastic materials in finite growth and deformation. *Journal of Elasticity*, 59, 175–193 (2000).

[35] Epstein, M. and Maugin, G. Thermomechanics of volumetric growth in uniform bodies. *International Journal of Plasticity*, 16, 951–978 (2000).

[36] DiCarlo, A. and Quiligotti, S. Growth and balance. *Mechanics Research Communications*, 29, 449–456 (2002).

[37] Lubarda, V. A. and Hoger, A. On the mechanics of solids with a growing mass. *International Journal of Solids and Structures,* 39, 4627–64 (2002).

[38] Haughton, D. M. and Ogden, R. W. On the incremental equations in non-linear elasticity-II. Bifurcation of pressurized spherical shells. *Journal of Mechanics and Physics of Solids,* 26, 111–138 (1978).

[39] Scott, N. H. The incremental bulk modulus, Young's modulus and Poisson's ratio in nonlinear isotropic elasticity: physically reasonable response. *Mathematics and Mechanics of Solids*, 12, 526 (2007).

[40] Perko, L. *Differential Equations and Dynamical Systems*. Springer, New York, 2001.